ELSEVIER

Biochimica et Biophysica Acta 1459 (2000) 230–238

BIOCHIMICA ET BIOPHYSICA ACTA

BBA

www.elsevier.com/locate/bba

Biophysical and structural characterization of proton-translocating NADH-dehydrogenase (complex I) from the strictly aerobic yeast *Yarrowia lipolytica*

Rogieh Djafarzadeh [a], Stefan Kerscher [a], Klaus Zwicker [a], Michael Radermacher [b], Martin Lindahl [b], Hermann Schägger [a], Ulrich Brandt [a,*]

[a] *Universitätsklinikum Frankfurt, Institut für Biochemie I, Zentrum der Biologischen Chemie, D-60590 Frankfurt am Main, Germany*

[b] *Max-Planck-Institut für Biophysik, Abt. Strukturbiologie, D-60528 Frankfurt am Main, Germany*

Received 4 April 2000; received in revised form 7 June 2000; accepted 8 June 2000

Abstract

Mitochondrial proton-translocating NADH-dehydrogenase (complex I) is one of the largest and most complicated membrane bound protein complexes. Despite its central role in eukaryotic oxidative phosphorylation and its involvement in a broad range of human disorders, little is known about its structure and function. Therefore, we have started to use the powerful genetic tools available for the strictly aerobic yeast *Yarrowia lipolytica* to study this respiratory chain enzyme. To establish *Y. lipolytica* as a model system for complex I, we purified and characterized the multisubunit enzyme from *Y. lipolytica* and sequenced the nuclear genes coding for the seven central subunits of its peripheral part. Complex I from *Y. lipolytica* is quite stable and could be isolated in a highly pure and monodisperse state. One binuclear and four tetranuclear iron–sulfur clusters, including N5, which was previously known only from mammalian mitochondria, were detected by EPR spectroscopy. Initial structural analysis by single particle electron microscopy in negative stain and ice shows complex I from *Y. lipolytica* as an L-shaped particle that does not exhibit a thin stalk between the peripheral and the membrane parts that has been observed in other systems.

Keywords: Mitochondria; Complex I; Yeast; Iron–sulfur cluster; Single particle analysis; EPR spectroscopy

1. Introduction

Mitochondrial NADH-dehydrogenase (EC 1.6.99.3, complex I) is among the largest and most complicated membrane bound multiprotein complexes known (see [1] and other reviews in this special issue on complex I). It links the electron transfer from NADH to ubiquinone with the translocation of four protons across the inner membrane [2,3]. Despite of its central role in eukaryotic oxidative phosphorylation and its involvement in a broad range of human disorders [4,5], little is known about its structure and function. A major reason for this is that the application of molecular genetics has been limited by the fact that the organism best suited for

Abbreviations: dNADH, deamino-NADH; HAR, hexamine-ruthenium(III)-chloride; NBQ, 2-*n*-nonyl-ubiquinone; PCR, polymerase chain reaction; SDS–PAGE, sodium dodecyl-sulfate polyacrylamide gel electrophoresis

* Corresponding author. Universitätsklinikum Frankfurt, Institut für Biochemie I, Zentrum der Biologischen Chemie, Theodor-Stern-Kai 7, Haus 25 B, D-60590 Frankfurt am Main, Germany. Fax: +49-69-6301-6970;
E-mail: brandt@zbc.klinik.uni-frankfurt.de

0005-2728/00/$ – see front matter
PII: S0005-2728(00)00154-7

this purpose, the fermentative yeast *Saccharomyces cerevisiae*, does not contain complex I [6]. Therefore, we have established the strictly aerobic yeast *Yarrowia lipolytica* as a model system to study the structure and function of complex I. *Y. lipolytica* combines the availability of the genetic tools that have made yeast genetics so successful with rapid growth, constitutively high content of mitochondria [7] and a complex I that remains stable upon purification.

Mitochondrial complex I is composed of some 40 different subunits with a total molecular mass of nearly 1000 kDa. Most of the subunits are encoded by nuclear genes, whereas the seven most hydrophobic subunits are encoded and synthesized within the mitochondrion [8,9]. The enzymes from bovine heart [10,11] and the filamentous fungus *Neurospora crassa* [12] have been purified and characterized. One FMN [10] and a still not exactly defined number of iron–sulfur clusters [13] serve as prosthetic groups. A simpler version of complex I is also found in many bacteria, e.g. *Escherichia coli*, *Paracoccus denitrificans*, *Rhodobacter capsulatus* and *Thermus thermophilus* (see [14] for a recent review). While powerful genetic techniques are available for several of these organisms, bacterial complex I tends to be very unstable and variable in content. Moreover, *Escherichia coli* complex I, the only bacterial enzyme that could be purified so far [15], is less conserved and seems to be functionally quite different as it pumps sodium ions in addition or instead of protons [16].

As a basis for our novel approach, we report the purification, enzymological characterization and biophysical analysis of complex I from *Yarrowia lipolytica*. The genes for those seven nuclear coded subunits forming the central part of the hydrophilic domain were cloned and sequenced. An initial structural analysis by single particle electron microscopy in ice demonstrates the suitability of the preparation for high resolution structural studies.

2. Materials and methods

2.1. Yeast growth and preparation of mitochondrial membranes

Y. lipolytica wild-type (strain E150) was grown at 30°C in a 50-l fermenter aerated at 50 l/h. The medium contained (w/v) 2% glucose, 2% bactopeptone and 1% yeast extract. Approximately 2 kg cells (wet mass)/50 l were harvested during late exponential growth phase after 14–16 h by centrifugation for 10 min at $5000\times g$. The cells were washed with water and stored at −80°C. All further steps were carried out at 4°C. One hundred and fifty grams of cells were resuspended in 300 ml 20 mM Na/MOPS, 400 mM sucrose and 1 mM EDTA, pH 7 and disrupted by a single pass through a Gaulin laboratory homogenizer at 500 MPa. Cell debris was removed by centrifugation for 30 min at $5000\times g$ and the membrane fraction consisting mostly of mitochondrial membranes was obtained by centrifugation for 1 h at $100\,000\times g$.

2.2. Cloning and sequencing

The nuclear genes coding for the seven highly conserved, central subunits of the peripheral part of complex I from *Y. lipolytica* were all cloned by the same general strategy: peptide sequences highly conserved among *Neurospora crassa, Bos taurus* and *Paracoccus denitrificans* were identified by sequence alignments using the GCG program CLUSTAL (HUSAR, DKFZ, Heidelberg, Germany). Degenerate primers were deduced by reverse translation and used for PCR on genomic DNA from haploid strain E150. The following degenerate primers were used to generate PCR-probes for the central complex I genes (forward primer/reverse primer): *NUAM*, CTIACIATIGAYGGNCAYAARG/GTYTTRTCRTTDATCCAYTCYTC; *NUBM*, CCITGYACIGTIGARGARGARATG/CKRCAIGGIGTRCAYTGICCRC; *NUCM*, CARGC IYTICCNTAYTTYG/RTCIACYTCICCRAANAC; *NUGM*, GCIAAYTGGTAYGARMG NG/GICCYTCRAANCCRTARTC; *NUHM*, CCIATGMGIGTITAYGARGTNGC/CAIGCICCIARRCAYTCNACY; *NUIM*, ATHTAYTAYCCITTYGARAARGG/CARTADATRCAYTTNGTCATRTC; *NUKM*, ACITTYGGIYTIGCITGYTGYGC/GGRCAICCIGGIACRTADATYTC. PCR products were subcloned into pCR2.1 (Invitrogen), verified by sequencing and used to screen an ordered genomic library from strain E150 [7]. Positive clones were sequenced in both directions using an ABI 310 genetic analyzer (PE Applied Biosystems). The genes were named according to the established nomenclature for mitochondrial complex

I from other organisms (the name of the homologous bovine subunit and the accession number for the EMBL database are given in brackets): *NUAM_YARLI* (75 kDa; AJ249781), *NUBM_YARLI* (51 kDa, 249782), *NUCM_YARLI* (49 kDa, AJ249783), *NUGM_YARLI* (30 kDa, AJ249784), *NUHM_YARLI* (24 kDa, AJ250338), *NUKM_YARLI* (PSST, AJ250340) *NUIM_YARLI* (TYKY, AJ250339).

2.3. Analytical methods

Protein was determined according to a modified Lowry protocol [17]. Redox spectra of cytochromes were recorded on a Shimadzu UV-300 spectrophotometer using reported extinction coefficients [18].

Low temperature X-band EPR-spectra were obtained on a Bruker ESP 300E spectrometer equipped with a liquid helium continuous flow cyrostat, ESR 900 from Oxford Instruments. The samples were mixed with NADH in the EPR tube and frozen in liquid nitrogen after 30 s reaction time. For all spectra, the same set of instrument parameters was used: microwave frequency 9.48 GHz, center field 345 mT, sweep width 70 mT, sweep time 167.8 s, time constant 163.84 ms, modulation frequency 100 kHz, modulation amplitude 1 mT. Spectra were accumulated five times and corrected for a baseline (buffer without complex I) recorded under the same conditions. Tricine SDS–PAGE was performed according to Schägger and von Jagow [19].

2.4. Determination of catalytic activity

Deamino-NADH (dNADH) was used to assay complex I, as it is not used as a substrate by the alternative NADH-dehydrogenase. dNADH:NBQ activity at 60 μM NBQ and 100 μM dNADH was measured using a Shimadzu UV-300 spectrophotometer in the dual-wavelength mode by following dNADH-oxidation at 340–400 nm ($\varepsilon = 6.10$ mM^{-1} cm^{-1}) and 30°C [18]. Thirty to 50 μg protein/ml of mitochondrial membranes or fractions from different preparation steps were used for this assay. For the determination of Michaelis–Menten parameters, the concentration of the substrates was varied in the appropriate range.

Inhibitor-insensitive dNADH:HAR activity was measured using a Shimadzu UV-300 spectrophotometer in the dual-wavelength mode by following dNADH-oxidation at 340–400 nm ($\varepsilon = 6.10$ mM^{-1} cm^{-1}) and 30°C [20].

2.5. Purification of complex I

All preparation steps were performed at 4°C. Mitochondrial membranes (20 mg total protein/ml) were suspended with 0.2 g lauryl maltoside/g protein in 100 ml of 50 mM NaCl, 1 mM EDTA and 20 mM Na/MOPS, pH 7.0 and centrifuged for 90 min at $100\,000 \times g$. The supernatant contained water-soluble enzymes and most of mitochondrial complex V. The sediment was resuspended to 20 mg/ml protein in 0.75 g lauryl maltoside/g protein, 50 mM NaCl, 1 mM EDTA and 20 mM Na/MOPS, pH 7.0 and centrifuged again at $100\,000 \times g$ for 90 min. The sediment contained most of mitochondrial complex IV, some complex III and a minor fraction of complex I. The supernatant containing most of complex I was adjusted to 75 mM NaCl and 2% (w/v) lauryl maltoside were added before application onto a 150-ml DEAE-Biogel A (Bio-Rad) column equilibrated with 75 mM NaCl, 0.05% lauryl maltoside, 1 mM EDTA and 25 mM Na/MOPS, pH 7.0 at a flow rate of 2.5 ml/min. The column was washed with one volume of 100 mM NaCl, 0.1% lauryl maltoside, pH 7.0 and complex I was eluted with 200 mM NaCl, 0.25% lauryl maltoside, 1 mM EDTA and 25 mM Na/MOPS, pH 7.0. Fractions containing dNADH:NBQ oxidoreductase activity were pooled, concentrated by centrifugation through Centricon 30 cartridges (Millipore), filtered through a 0.2-μM nylon thread filter (Roth) and applied to a 21.5 mm $\times 60$ cm TSKgel G4000SW column (Toso-Haas) equilibrated with 0.1% lauryl maltoside and 100 mM NaCl, 1 mM EDTA and 25 mM Na/MOPS, pH 7.0. Chromatography in the same buffer was performed in a Beckman Biosys 2000 System at a flow rate of 2.5 ml/min. *Y. lipolytica* complex I eluted as a dominant peak detected at 280 nm, which was identified as the monomeric form of the pure enzyme with a molecular mass close to 1000 kDa. Fractions containing complex I were pooled, concentrated and stored in liquid nitrogen. Typically, about 5 mg of purified enzyme were obtained from 2000 mg of mitochondrial membranes.

2.6. Protein sequencing

For amino-terminal sequencing, mitochondrial membranes were dissolved in 2% lauryl maltoside and 500 mM aminocaproic acid and separated by two-dimensional BN/SDS–PAGE [21]. After transfer onto a polyvinylidene-difluoride membrane, individual subunits were sequenced by automated Edman degradation, in an Applied Biosystems 473 A pulsed-liquid protein sequencer.

2.7. Negative stain electron microscopy and image processing

Complex I was diluted to a concentration of 0.03 mg/ml. A 5-μl amount of the specimen was applied to holey carbon coated grids covered with an additional thin carbon layer and stained with 1% uranyl acetate. Images were recorded under low-dose conditions in a Phillips CM12 microscope at 100 kV acceleration voltage at 45 000× magnification and a defocus of approximately 0.8 μm. Films were developed in full strength D19 (Kodak). Selected micrographs were scanned with a Zeiss SCAI flatbed scanner using a stepsize of 7 μm and subsequently binned down to 21 μm, corresponding to a pixel size of 4.7Å on the specimen scale. Image processing was performed using the programs SPIDER and WEB [22,23].

Nine hundred particles showing approximate L-shape were initially selected from 21 micrographs. After contrast normalization, alignment was performed by rotational alignment of the auto correlation functions [24], followed by translational and rotational alignment in direct space [25]. For classification, the aligned images were analyzed with correspondence analysis [26,27], and classified using the *dynamic clouds* algorithm [28] followed by hierarchical ascendent classification [29]. This resulted in two major classes, which apparently corresponded to particles with opposite sides facing the carbon support. The images in one of the classes were mirrored, realigned with the images of the second class and averaged. The resulting average (Fig. 3 top) contains 750 images. For resolution determination, the data set was split in half, two averages were calculated and compared by Fourier ring correlation [30,31] using as cutoff value five times the noise correlation (FRC_5) or three times the noise correlation (FRC_3) [32].

2.8. Cryo-electron microscopy and image processing

For cryo-electron microscopy, the specimen was diluted to 0.1 mg/ml and then applied to holey carbon coated grids covered with an additional thin carbon layer and rapidly frozen in liquid ethane. Microscopy was carried out on a Phillips CM120 at 120 kV acceleration voltage and a magnification of 60 000× and a defocus value of 2.1 μm. From 19 micrographs, 771 images were selected and processed using the same methods as for the stained specimen. After classification, two major classes, corresponding to particles facing the support with opposite sides could again be distinguished. The members of one class were mirrored and realigned as described above and an average consisting of 479 particles was calculated (Fig. 3 bottom).

3. Results

3.1. Cloning and sequencing of the seven nuclear genes coding for the central subunits of peripheral part of complex I from Y. lipolytica

We have cloned and sequenced the *Y. lipolytica* genes, encoding the seven highly conserved, nuclear encoded subunits of complex I. These subunits harbor one non-covalently bound FMN and six to seven iron–sulfur clusters. A synopsis of the characteristic features of these central proteins of complex I from *Y. lipolytica* is presented in Table 1. The length of the deduced protein sequences were comparable to the homologous subunits from other species. No introns were found in any of the open reading frames. In five cases, the determination of N-terminal sequences from the mature proteins allowed for direct identification of the site of processing following import to the mitochondrial matrix space (Table 1, Fig. 1). The length of the presequences varies between 18 and 34 amino acids and all five processing sites exhibited an arginine in position −3 as has been reported for many mitochondrial proteins [33].

All seven proteins are well conserved between *Y. lipolytica*, *N. crassa*, *B. taurus*, *P. denitrificans*,

Table 1
Characteristic features of the seven nuclear coded central subunits of *Y. lipolytica* complex I

Gene symbol	Subunit in bovine heart complex I	Amino acids of open reading frame	Amino acids of mature protein	M_r of mature apoprotein	Processing site[a]	Conserved iron–sulfur cluster binding motifs[b]	Prosthetic groups (bovine)[b]
NUAM	75 kDa	728	694	75 195	A<u>R</u>RL|AEIE	D-(x)$_6$-E-(x)$_8$-C-(x)$_{10}$-C-(x)$_{10}$-CxxC-(x)$_{13}$-C-(x)$_{35}$-CxxCxxxxxC-(x)$_{40}$-CxxCxxC-(x)$_{44}$-CP	N1b, N4, N5
NUBM	51 kDa	488	470	51 657	S<u>R</u>GF|ATTQ	CxxCxxC-(x)$_{39}$-C	FMN, N3
NUCM	49 kDa	466	444	49 942	A<u>R</u>YM|ATTA		
NUGM	30 kDa	281	251	29 225	A<u>R</u>AA|EAAP		
NUHM	24 kDa	243				CxxxxC-(x)$_{35}$-CxxxC	N1a
NUIM	TYKY	229				-CxxCxxCxxxCP-(x)$_{27}$-CxxCxxCxxxCP	N2?
NUKM	PSST	210	183	20 425	T<u>R</u>AY|SAPA	CCxxE-(x)$_{60}$-C-(x)$_{29}$-CP	N2?

[a]A vertical line marks the start of the mature protein as determined by Edman degradation. The −3 arginine is underlined.
[b]N1a and N1b are binuclear clusters, N2, N3, N4 and N5 are tetranuclear clusters [13]. The location of center N2 is controversial.

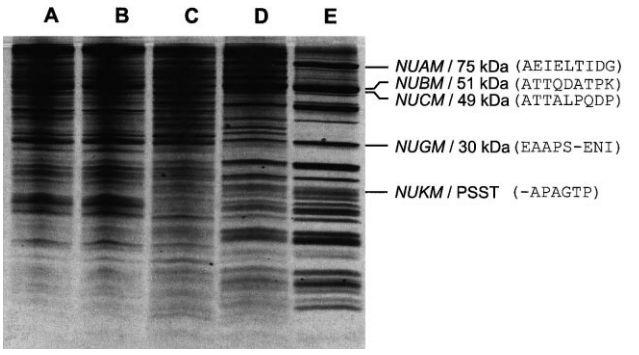

Fig. 1. Stages of complex I purification and N-terminal sequences of five central subunits. Silver-stained tricine SDS–PAGE of isolated complex I and different stages of preparation was performed according to Schägger and von Jagow [19]. The protein samples (5 μg total protein, see Table 1) were incubated for 30 min at 35°C in 4% SDS (w/v), 2% mercaptoethanol, 10% glycerol, 0.01% Serva blue G, 50 mM Tris/HCl, pH 7.0. (A) membranes; (B) sediment of pre-extraction; (C) supernatant of extraction; (D) Biogel A-pool; (E) TSKgel G4000SW-pool. See also Table 3.

R. capsulatus and *E. coli*. This is illustrated in Table 2 by comparing sequence similarity values calculated from pairwise alignments of the translation products of the complete open reading frames. The similarity values for the subunits of the *E. coli* enzyme are significantly lower than for the two other bacterial species. This may be related to the recent observation that complex I from *E. coli* translocates sodium ions instead or in addition to protons [16].

3.2. Purification and general characterization of complex I from Y. lipolytica

The progress of a typical preparation of complex I from *Y. lipolytica* mitochondrial membranes is summarized in Table 3 and illustrated by SDS–PAGE of the different stages of purification in Fig. 1. The progress of purification was monitored by the complex I-specific substrate deamino-NADH because it does not react with alternative NADH-dehydrogenases in *Y. lipolytica* [7]. Hexamine-ruthenium(III)-chloride (HAR) was used as an artificial electron acceptor; in contrast to the physiological acceptor ubiquinone, its reactivity with complex I does not depend on the presence of detergents and the lipidation of complex I [34]. Judged by this activity, complex I was enriched 30-fold in the pooled fractions of the TSKgel G4000SW column in comparison to solubi-

Table 2
Sequence similarity (%) of central subunits of the peripheral part of complex I from various organisms to subunits from *Y. lipolytica*[a]

Subunit	*Neurospora crassa*	*Bos taurus*	*Paracoccus denitrificans*	*Rhodobacter capsulatus*	*Escherichia coli*
NUAM/75 kDa	73	63	57	59	39
NUBM/51 kDa	79	75	71	72	50
NUCM/49 kDa	77	75	66	68	51
NUGM/30 kDa	70	61	57	58	40
NUHM/24 kDa	67	64	46	49	45
NUIM/TYKY	77	66	77	75	43
NUKM/PSST	78	72	72	71	52

[a]Values were calculated using the GCG program GAP, HUSAR, DKFZ, Heidelberg, Germany, using a gap creation penalty of 8 and a gap extension penalty of 2.

lized mitochondrial membranes and the yield was near 10%. No contaminations by other respiratory chain complexes could be detected by SDS–PAGE of the purified enzyme (Fig. 1). Optical spectra at 400–500 nm of the air oxidized preparation revealed minor residual contaminations by cytochrome *c* oxidase (data not shown). If required, this and other remaining impurities were removed by a second pass through the TSKgel G4000SW column, resulting in highly pure enzyme with a specific HAR activity up to 60 μmol min^{-1} mg^{-1}. After the first pass, the preparation exhibited a specific activity for deamino-NADH to nonylubiquinone (NBQ) of 0.7 μmol min^{-1} mg^{-1} at 30°C and pH 7.0. This activity could be fully inhibited by complex I inhibitors like rotenone, piericidin A and DQA [18]. Using the deamino-NADH to HAR activity as an internal standard, the specific activity after purification could be estimated to reflect a turnover number that was only 5–10% when compared to mitochondrial membranes. However, the addition of phospholipid to the purified enzyme resulted in an up to four-fold recovery of the quinone-reductase activity (data not shown). The K_m value for deamino-NADH was 15 ± 3 μM which is slightly lower than in mitochondrial membranes (26 ± 3 μM). The apparent K_m value for nonylubiquinone was decreased 2.5-fold upon purification from 20 ± 1 to 8 ± 1 μM.

3.3. EPR-spectroscopic analysis of iron–sulfur clusters

EPR-spectra of the isolated complex I from *Y. lipolytica* at 35 and 12 K were found to be similar to those reported earlier for the *N. crassa* enzyme [35]. Four Fe–S clusters could be detected (Fig. 2A) and were identified as the binuclear cluster N1, and the three tetranuclear clusters N2, N3 and N4 based on their similarity to the *N. crassa* enzyme (Table 4): at relatively high sample temperature (35 K) only the binuclear [2Fe–2S] cluster N1 could be detected. At lower temperature (12 K) the tetranuclear [4Fe–4S] clusters N2, N3 and N4 could be identified by their characteristic *g*-values.

At 5 K, the spectrum of an additional iron–sulfur cluster was detected with $g_z = 2.065$ (Fig. 2B). The g_x and g_y region of the spectrum could not be identified with certainty. With increasing microwave power up to 100 mW the signal of this iron–sulfur cluster became more and more pronounced indicating a very fast relaxation time. At 5 K, the half-saturation pa-

Table 3
Purification of *Y. lipolytica* complex

Fraction	Protein		dNADH/HAR activity		
	mg	%	μmol min^{-1}	%	μmol min^{-1} mg^{-1}
Solubilized mitochondria	2500	100	2940	100	1.2
Sediment of pre-extraction	1480	59	2550	87	1.7
Supernatant of extraction	530	21	1340	46	2.5
DEAE-Biogel A pool	33	1.3	610	21	19
TSKgel G4000SW pool	7	0.3	280	9.5	40

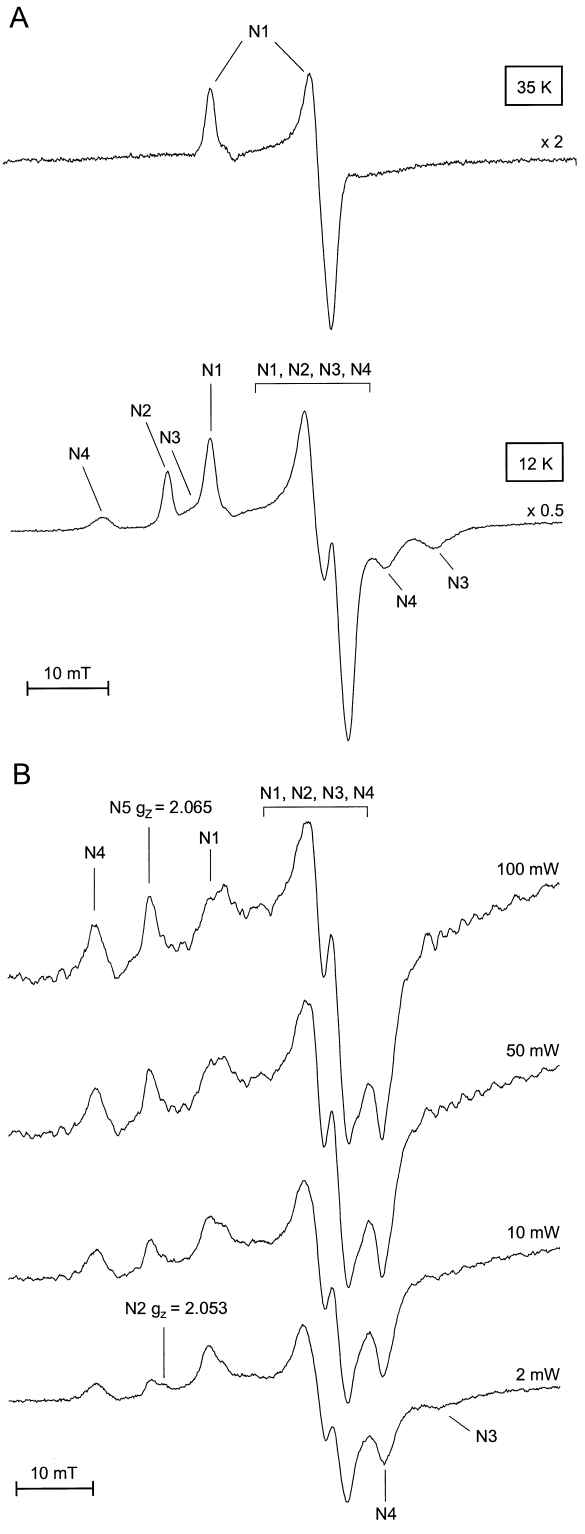

Fig. 2. EPR spectra of purified complex I from *Y. lipolytica*. A 6.2-mg/ml amount of complex I was reduced by adding 2.5 mM NADH. (A) EPR spectra at 35 and 12 K recorded with 2 mW microwave power. The EPR signatures of iron–sulfur clusters N1 to N4 were identified based on their similarity to the *N. crassa* enzyme [35]. (B) Series of 5 K EPR spectra covering a range of 2–100 mW microwave power. $P_{1/2}$ for iron–sulfur cluster N5 was estimated to be about 180 mW at this temperature. See Section 2 for other EPR parameters.

→

rameter $P_{1/2}$ was estimated to be 180 mW. These parameters are characteristic of an additional tetranuclear iron–sulfur cluster N5 that was previously found only in bovine heart complex I ($g_{z,y,x} = 2.07$, 1.93, 1.90 [13]). It should be stressed that this signal was observed with several different batches of protein and after one or two passes through the TSKgel G4000SW column. In samples examined, the intensity was the same relative to those of other iron–sulfur clusters. With increasing microwave power a significant enhancement of signals round $g = 1.93$ and 1.90 was observed that went essentially parallel with the g_z signal of cluster N5. We assume that this was due to the g_x and g_y signals of cluster N5, but an unambiguous assignment was impossible, because of an overlap with the spectrum of N4 that also exhibits increasing intensity between 10 and 100 mW of microwave power.

3.4. Single-particle electron microscopy

Preparations of complex I were analyzed as single particles by electron microscopy and image process-

Table 4
Compilation of g values for individual iron–sulfur clusters in complex I from *Y. lipolytica* (this work) and *N. crassa* [35]

Organism	Iron–sulfur cluster	g values		
		g_z	g_y	g_x
Y. lipolytica	N1	2.020	1.943	1.94
	N2	2.053	1.929	1.925
	N3	2.030	1.924	1.860
	N4	2.103	1.939	1.894
	N5	2.065	(1.93)	(1.90)
N. crassa	N1	2.019	1.935	1.933
	N2	2.051	1.925	1.916
	N3	2.044	1.928	1.867
	N4	2.098	1.920	1.884

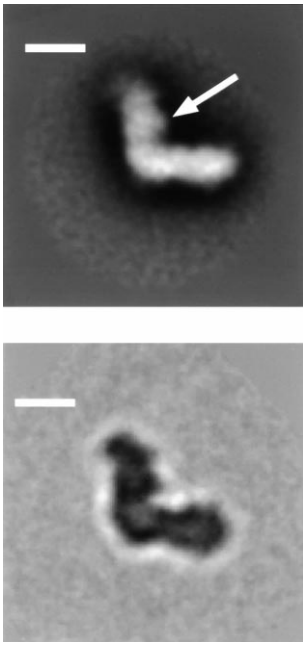

Fig. 3. Single-particle average of complex I from *Y. lipolytica*. Top: negatively stained particles, resolution FRC_5, 36 Å (FRC_3, 27 Å). Scale bar: 100 Å. The arrow indicates the position of the 49-kDa subunit which has been identified in *N. crassa* by monoclonal antibody binding [37]. Bottom: particles in ice, resolution FRC_5, 32 Å (FRC_3, 29 Å). Scale bar: 100 Å.

ing. Images from negatively stained specimens and from frozen hydrated specimens were analyzed.

The average image, calculated from 750 particles in negative stain (Fig. 3 top) revealed an L- or boot-shaped particle. Based on earlier studies of the *N. crassa* enzyme [36], the horizontal domain was identified as the membrane bound part and the vertical arm was assigned to the hydrophilic part projecting into the mitochondrial matrix space. This vertical arm revealed a protrusion (see arrow in the top of Fig. 3), which, for complex I of *N. crassa*, had been found to bind Fab fragments directed against the 49-kDa subunit [37].

Similar features can be seen in images of frozen hydrated particles of complex I from *Y. lipolytica* (Fig. 3 bottom). The average was calculated from 479 particles. The matrix part seemed to consist of two main features, the 49-kDa domain mentioned above and a second dense domain at the top of the arm. Near the cluster of the membrane domain, an indentation can be seen, which had also been apparent from negatively stained particles of bovine complex I. However, in contrast to projection images from frozen particles of bovine complex I [38], we could not observe the appearance of a stalk between the membrane domain and the peripheral arm in frozen hydrated preparations (Fig. 3 bottom).

4. Discussion

Our data represent a comprehensive characterization of proton-translocating NADH-dehydrogenase (complex I) from *Y. lipolytica*. The stability of this very large membrane bound multiprotein complex and the well developed genetics of this obligate aerobic yeast [39] make this organism an ideal model system for functional, structural and genetic analysis of eukaryotic complex I.

With respect to overall subunit composition and sequence homology of the seven nuclear coded central subunits, complex I from *Y. lipolytica* is very similar to the enzyme from the ascomycete *N. crassa* [1]. Also, all EPR detectable iron–sulfur clusters characterized earlier in the *N. crassa* complex were present in isolated *Y. lipolytica* complex I and exhibited very similar EPR signatures. However, at high microwave power and very low temperature, we could detect an additional very fast relaxing iron–sulfur cluster. Its *g*-values and relaxation properties were in the same range as reported for iron–sulfur cluster N5 that has been so far described only for the bovine complex [13]. As iron–sulfur cluster N5 had been found only in bovine submitochondrial particles and not in *Candida utilis* [40] or plant mitochondria [41], it was questioned whether this cluster is a genuine component of complex I [42]. Our finding that purified complex I from *Y. lipolytica* contains this redox center makes this argument obsolete and identifies center N5 as a true component of this respiratory chain complex. N5 may have been missed in other systems due to its very fast relaxation.

Purified complex I from *Y. lipolytica* also proves to be well suited for structural studies. Our initial analysis by single particle electron microscopy revealed no significant difference between molecules in ice and in negative stain. The L-shaped structure is very similar to the structural model derived from negatively stained particles of the *N. crassa* enzyme [37]. This is in contrast to bovine complex I that looks similar to the fungal enzyme in negatively stained particles, but

exhibits a thin stalk connecting the peripheral and the membrane part of the complex in ice [38]. We have found no indication for such a thin stalk in the *Y. lipolytica* enzyme. Further structural studies including attempts to crystallize complex I from *Y. lipolytica* are in progress.

The work presented here forms the basis for structure/function analysis of complex I by efficient site-directed mutagenesis of complex I from *Y. lipolytica*. This approach has already proven to be useful and the first functionally deficient mutants have been characterized (Ahlers et al., submitted for publication).

Acknowledgements

We would like to thank T. Ruiz for extensive help with the electron microscopy. This work was supported by grant SFB 472 of the Deutsche Forschungsgemeinschaft, the Fonds der Chemischen Industrie, and a Marie Curie research training grant (BIO4-CT98-5026) by the European Union to M.L.

References

[1] A. Videira, Biochim. Biophys. Acta 1364 (1998) 89–100.
[2] M.K.F. Wikström, FEBS Lett. 169 (1984) 300–304.
[3] H. Weiss, T. Friedrich, J. Bioenerg. Biomembr. 23 (1991) 743–771.
[4] A.H. Schapira, Biochim. Biophys. Acta 1364 (1998) 261–270.
[5] B.H. Robinson, Biochim. Biophys. Acta 1364 (1998) 271–286.
[6] T. Ohnishi, K. Kawaguchi, B. Hagihara, J. Biol. Chem. 241 (1966) 1797–1806.
[7] S. Kerscher, J.G. Okun, U. Brandt, J. Cell Sci. 112 (1999) 2347–2354.
[8] A. Chomyn, P. Mariottini, M.W.J. Cleeter, C.I. Ragan, A. Matsuno-Yagi, Y. Hatefi, R.F. Doolittle, G. Attardi, Nature 314 (1985) 592–597.
[9] A. Chomyn, M.W.J. Cleeter, C.I. Ragan, M. Riley, R.F. Doolittle, G. Attardi, Science 234 (1986) 614–618.
[10] Y. Hatefi, J.S. Rieske, Methods Enzymol. 10 (1967) 235–239.
[11] M. Finel, J.M. Skehel, S.P.J. Albracht, I.M. Fearnley, J.E. Walker, Biochemistry 31 (1992) 11425–11434.
[12] H. Weiss, T. Friedrich, G. Hofhaus, D. Preis, Eur. J. Biochem. 197 (1991) 563–576.
[13] T. Ohnishi, Biochim. Biophys. Acta 1364 (1998) 186–206.
[14] T. Yagi, T. Yano, S. Di Bernardo, A. Matsuno-Yagi, Biochim. Biophys. Acta 1364 (1998) 125–133.
[15] H. Leif, V.D. Sled, T. Ohnishi, H. Weiss, T. Friedrich, Eur. J. Biochem. 230 (1995) 538–548.
[16] J. Steuber, C. Schmid, M. Rufibach, P. Dimroth, Mol. Microbiol. 35 (2000) 428–434.
[17] O.H. Lowry, N.R. Rosebrough, A.L. Farr, R.J. Randall, J. Biol. Chem. 193 (1951) 265–275.
[18] J.G. Okun, P. Lümmen, U. Brandt, J. Biol. Chem. 274 (1999) 2625–2630.
[19] H. Schägger, G. von Jagow, Anal. Biochem. 166 (1987) 368–379.
[20] V.D. Sled, A.D. Vinogradov, Biochim. Biophys. Acta 1143 (1993) 199–203.
[21] H. Schägger, W.A. Cramer, G. von Jagow, Anal. Biochem. 217 (1994) 220–230.
[22] J. Frank, B. Shimkin, H. Dowse, Ultramicroscopy 6 (1981) 343–358.
[23] J. Frank, M. Radermacher, P. Penzcek, J. Zhu, Y. Li, M. Ladjadj, A. Leith, J. Mol. Biol. 161 (1996) 134–137.
[24] J. Frank, W. Goldfarb, D. Eisenberg, T.S. Baker, Ultramicroscopy 3 (1978) 283–290.
[25] M. Steinkilberg, H.J. Schramm, Hoppe-Seylers Z. Physiol. Chem. 361 (1980) 1363–1369.
[26] M. van Heel, J. Frank, Ultramicroscopy 6 (1981) 187–194.
[27] J. Frank, M.G. van Heel, J. Mol. Biol. 161 (1982) 134–137.
[28] E. Diday, Rev. Stat. Appl. 19 (1971) 19–34.
[29] J. Frank, Q. Rev. Biophys. 23 (1990) 281–329.
[30] W.O. Saxton, W. Baumeister, J. Microscopy 127 (1982) 127–138.
[31] M.G. van Heel, W. Keegstra, W. Schutter, E.F.J. van Bruggen, Life Chemistry Reports, Suppl. 1 (1982) 69–73.
[32] M. Radermacher, J. Electron Microsc. Tech. 9 (1988) 359–394.
[33] G. Schneider, S. Sjöling, E. Wallin, P. Wrede, E.G. Glaser, G. von Heijne, PROTEINS: Struct. Funct. Gen. 30 (1998) 49–60.
[34] V.D. Sled, A.D. Vinogradov, Biochim. Biophys. Acta 1141 (1993) 262–268.
[35] D.-C. Wang, S.W. Meinhardt, U. Sackmann, H. Weiss, T. Ohnishi, Eur. J. Biochem. 197 (1991) 257–264.
[36] G. Hofhaus, H. Weiss, K. Leonard, J. Mol. Biol. 221 (1991) 1027–1043.
[37] V. Guenebaut, R. Vincentelli, D. Mills, H. Weiss, K.R. Leonard, J. Mol. Biol. 265 (1997) 409–418.
[38] N. Grigorieff, J. Mol. Biol. 277 (1998) 1033–1046.
[39] G. Barth, C. Gaillardin, in: K. Wolf (Ed.), Non-Conventional Yeasts in Biotechnology, Springer, Berlin, 1996, pp. 313–388.
[40] S.P. Albracht, G. Dooijewaard, F.J. Leeuwerik, B.V. Swol, Biochim. Biophys. Acta 459 (1977) 300–317.
[41] P.R. Rich, W.D Bonner Jr., in: D. Lloyd, H. Degn, G.C. Hill (Eds.), Functions of Alternative Respiratory Oxidases, 1978, Pergamon Press, New York, pp. 61–68.
[42] S.P.J. Albracht, A.M.P. de Jong, Biochim. Biophys. Acta 1318 (1997) 92–106.